Supporting Information

A semi-synthetic kanglemycin shows *in vivo* efficacy against high-burden rifampicin resistant pathogens

Authors: James Peek[1], Jiayi Xu[2], Han Wang[3], Shraddha Suryavanshi[4], Matthew Zimmerman[3], Riccardo Russo[4], Steven Park[5], David S. Perlin[5], and Sean F. Brady[1*]

Author affiliations: [1]Laboratory of Genetically Encoded Small Molecules, The Rockefeller University, 1230 York Avenue, New York, NY 10065. [2]Tri-Institutional Therapeutics Discovery Institute, Belfer Research Building, 413 E 69th Street, New York, NY, 10021. [3]Center for Discovery and Innovation, Hackensack Meridian Health, 340 Kingsland Street, Nutley, NJ 07110. [4]Rutgers, the State University of New Jersey, International Center for Public Health, 225 Warren Street, Newark, NJ 07103. [5]Center for Discovery and Innovation, Hackensack Meridian Health, 111 Ideation Way, Nutley, NJ 07110.

***Corresponding Author:** Sean F. Brady

Contact: Laboratory of Genetically Encoded Small Molecules

The Rockefeller University

1230 York Avenue

New York, NY 10065

Phone: 212-327-8280

Fax: 212-327-8281

Email: sbrady@rockefeller.edu

Table of Contents

1. **Table S1. Pharmacokinetic properties of Kang A, J4, and KZ**
2. **Table S2. Comparison of bacterial burdens in mouse kidneys infected with MRSA strain COL following treatment with Kang A, J4, KZ, or Rif**
3. **Figure S1. Complete collection of aliphatic amines used in the synthesis of Kang amides**
4. **Figure S2. Complete collection of cyclic amines used in the synthesis of Kang amides**
5. **Figure S3. Complete collection of aromatic amines used in the synthesis of Kang amides**
6. **Figure S4. Complete collection of carboxylic acid amines used in the synthesis of Kang amides**
7. **Figure S5. Complete collection of phosphate mimic amines used in the synthesis of Kang amides**
8. **Figure S6. Complete collection of sugar amines used in the synthesis of Kang amides**
9. **Figure S7. Complete collection of Phe/Trp/Try/His analogue amines used in the synthesis of Kang amides**
10. **Figure S8. Complete collection of amines uses in the synthesis C-3/C-4 Kang derivatives**
11. **Table S3. Comparison of bacterial burdens in mouse kidneys infected with *S. aureus* ATCC 12600 carrying an S486L RNAP mutation following treatment with KZ or Rif**
12. **Figure S9. Calibration curve used to determine the concentration of Kang amides**
13. **Figure S10. UPLC traces and UV spectra of purified Kang A, J4, and KZ**
14. **Figure S11. Mass fragmentation analysis of Kang A, J4, and KZ**
15. **Figure S12. HRMS and NMR data used to verify the structures of J4 and KZ**
16. **Table S4. ^{1}H and ^{13}C chemical shifts of Kang A, J4, and KZ**
17. **Figure S13. ^{1}H NMR spectrum of Kang A in CD_2Cl_2**
18. **Figure S14. ^{13}C NMR spectrum of Kang A in CD_2Cl_2**
19. **Figure S15. HMQC spectrum of Kang A in CD_2Cl_2**
20. **Figure S16. HMBC spectrum of Kang A in CD_2Cl_2**
21. **Figure S17. COSY spectrum of Kang A in CD_2Cl_2**
22. **Figure S18. ^{1}H NMR spectrum of J4 in $CDCl_3$**
23. **Figure S19. ^{13}C NMR spectrum of J4 in $CDCl_3$**
24. **Figure S20. HSQC NMR spectrum of J4 in $CDCl_3$**
25. **Figure S21. HMBC NMR spectrum of J4 in $CDCl_3$**

26. Figure S22. COSY NMR spectrum of J4 in $CDCl_3$

27. Figure S23. ^{1}H NMR spectrum of KZ in DMSO-d_6

28. Figure S24. ^{13}C NMR spectrum of KZ in DMSO-d_6

29. Figure S25. HSQC NMR spectrum of KZ in DMSO-d_6

30. Figure S26. HMBC NMR spectrum of KZ in DMSO-d_6

31. Figure S27. COSY NMR spectrum of KZ in DMSO-d_6

Table S1. Pharmacokinetic properties of Kang A, J4, and KZ. NA, not applicable; BLQ, below limit of quantification.

	IV	PO	IP
Kang A			
Dose (mg/kg)	5	5	5
AUC-inf (hr*ng/mL)	10320	BLQ	706
Dose corrected AUG	2064	BLQ	141
Bioavailability (%)	NA	BLQ	6.84
Half-life (hr)	0.84	NA	NA
k elimination (hr^{-1})	0.72	NA	NA
Vol. distribution (L/kg)	0.67	NA	NA
Clearance (mL/kg*hr)	487	NA	NA
J4			
Dose (mg/kg)	5	5	5
AUC-inf (hr*ng/mL)	7762	48.7	3007
Dose corrected AUG	1552	9.73	601
Bioavailability (%)	NA	0.63	38.7
Half-life (hr)	1.09	NA	NA
k elimination (hr^{-1})	0.51	NA	NA
Vol. distribution (L/kg)	1.28	NA	NA
Clearance (mL/kg*hr)	651	NA	NA
KZ			
Dose (mg/kg)	5	5	5
AUC-inf (hr*ng/mL)	54150	2923	14843
Dose corrected AUG	10830	585	2969
Bioavailability (%)	NA	5.4	27.4
Half-life (hr)	1.17	NA	NA
k elimination (hr^{-1})	0.55	NA	NA
Vol. distribution (L/kg)	0.17	NA	NA
Clearance (mL/kg*hr)	94.0	NA	NA

Table S2. Comparison of bacterial burdens in mouse kidneys infected with MRSA strain COL following treatment with Kang A, J4, KZ or Rif. Efficacy of compounds was evaluated in a neutropenic murine acute peritonitis/septicemia model. Infected mice received IP injections of drug (15 mg/mL) or vehicle (5% DMA plus 30% Captisol) at 2, 4 and 8 hours post infection. Bacterial burdens in kidneys were determined at 24 hrs post-infection. Limit of detection for burden quantification was calculated as 100 CFU/g of kidney. Log change in burden was calculated relative to the vehicle treated group.

Treatment	Mice	Average log CFU/g kidney	Average/Group	Log change in burden
Vehicle (5% DMA plus 30% Captisol)	1	5.2	5.6	0.0
	2	6.1		
	3	5.9		
	4	5.5		
	5	5.6		
	6	5.1		
Kang A (15 mg/kg)	1	3.8	3.8	-1.8
	2	4.1		
	3	4.1		
	4	3.8		
	5	2.6		
	6	4.6		
J4 (15 mg/kg)	1	2.6	4.1	-1.5
	2	4.7		
	3	3.8		
	4	5.0		
	5	4.0		
	6	4.7		
KZ (15 mg/kg)	1	sterilized	0.0	-5.6
	2			
	3			
	4			
	5			
	6			
Rif (15 mg/kg)	1	sterilized	0.0	-5.6
	2			
	3			
	4			
	5			
	6			

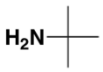 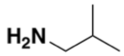  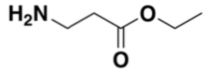 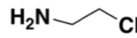 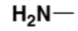 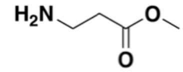

	J5	C10	D4	E4	N1	C23	E3
Expected mass (M - H+)	1035.5	1035.5	1007.4	1079.5	1041.4	993.4	1065.4
Experimental mass	1035.5	1035.5	1007.4	1079.5	1041.4	993.4	1065.4
WT	0.000061	0.0039	0.0039	0.0039	0.0039	0.016	0.016
H481Y	>64	>64	>64	>64	>64	>64	>64
S486L	16	16	4	64	16	16	16

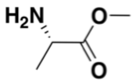 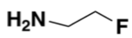 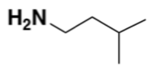 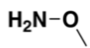 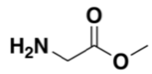 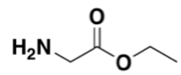 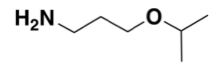

	J2	N36	D2	E1	E2	J6	N7
Expected mass (M - H+)	1065.4	1025.4	1049.5	1009.4	1051.4	1065.4	1079.5
Experimental mass	1065.4	1025.4	1049.5	1009.4	1051.4	1065.4	1079.5
WT	0.016	0.016	0.063	0.063	0.063	0.063	0.063
H481Y	64	64	>64	>64	>64	>64	>64
S486L	4	4	16	16	16	16	16

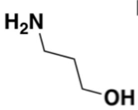 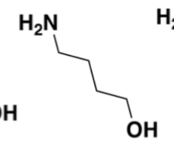 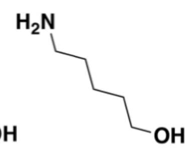 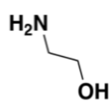 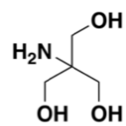

	G1	G2	G3	J1	G5
Expected mass (M - H+)	1037.5	1051.5	1065.5	1023.4	1083.5
Experimental mass	1037.5	1051.5	1065.5	1023.4	1083.5
WT	1	1	1	1	16
H481Y	>64	>64	>64	>64	>64
S486L	64	64	64	>64	>64

Round 2: J5 subscreen

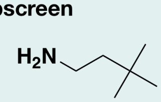 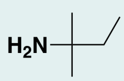 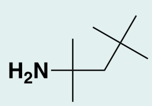 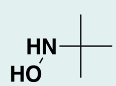 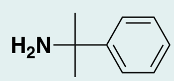 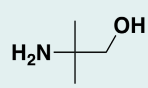 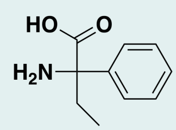

	N6	N39	N40	N41	N43	N42	N44
Expected mass (M - H+)	1063.5	1049.5	1091.5	1051.5	1097.5	1051.5	1141.5
Experimental mass	1063.5	1049.5	1091.5	1051.5	1097.5	1051.5	1141.5
WT	0.063	0.063	0.063	0.063	0.25	1	1
H481Y	>64	>64	>64	>64	>64	>64	>64
S486L	4	4	4	4	16	64	64

Figure S1. Complete collection of aliphatic amines used in the synthesis of Kang amides. Aliphatic amines were screened over two rounds of synthesis. The first round of synthesis broadly sampled this class of amines, while the second round utilized amines structurally related to J5, which yielded the most potent amide in the initial round of screening. The identity of each synthesized amide was verified by LC/MS. Expected and experimental masses are indicated. MIC values (µg/mL) are shown for the amides generated from each amine against wild-type and rifampicin resistant (H481Y and S486L) *S. aureus* strains.

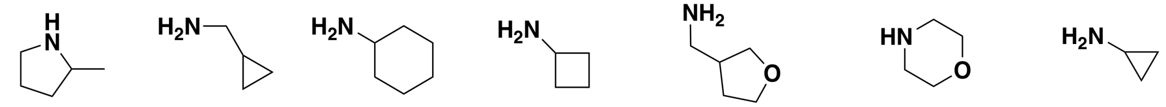

	N29	B1	C11	J7	B4	C4	C9
Expected mass (M - H+)	1047.5	1033.5	1061.5	1033.5	1063.5	1049.5	1019.4
Experimental mass	1047.5	1033.5	1061.5	1033.5	1063.5	1049.5	1019.4
WT	0.00098	0.00098	0.0039	0.0039	0.016	0.016	0.016
H481Y	>64	>64	>64	>64	64	>64	>64
S486L	4	16	64	16	4	16	16

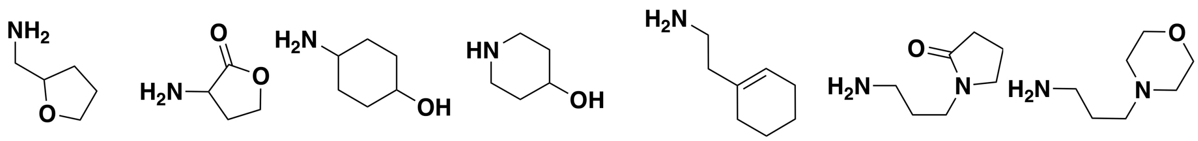

	B3	C20	B2	C12	N9	N10	N11
Expected mass (M - H+)	1063.5	1063.4	1077.5	1063.5	1087.5	1104.5	1106.5
Experimental mass	1063.5	1063.4	1077.5	1063.5	1087.5	1104.5	1106.5
WT	0.063	0.063	1	1	1	1	1
H481Y	64	>64	>64	>64	>64	>64	>64
S486L	4	16	64	64	16	64	>64

Round 2: N29 subscreen

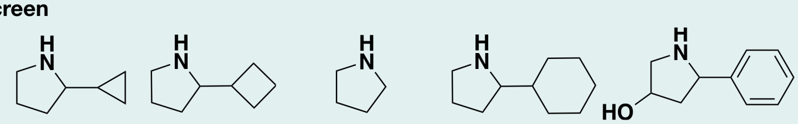

	C5	C6	N28	C7	C8
Expected mass (M - H+)	1073.5	1087.5	1033.5	1115.5	1125.5
Experimental mass	1073.5	1087.5	1033.5	1115.5	1125.5
WT	0.00024	0.016	0.016	0.25	0.25
H481Y	>64	>64	>64	>64	>64
S486L	16	16	16	64	16

Figure S2. Complete collection of cyclic amines used in the synthesis of Kang amides. Cyclic amines were screened over two rounds of synthesis. The first round of synthesis broadly sampled this class of amines, while the second round utilized amines structurally related to N29, which yielded one of the most potent amides in the initial round of screening. The identity of each synthesized amide was verified by LC/MS. Expected and experimental masses are indicated. MIC values (μg/mL) are shown for the amides generated from each amine against wild-type and rifampicin resistant (H481Y and S486L) *S. aureus* strains.

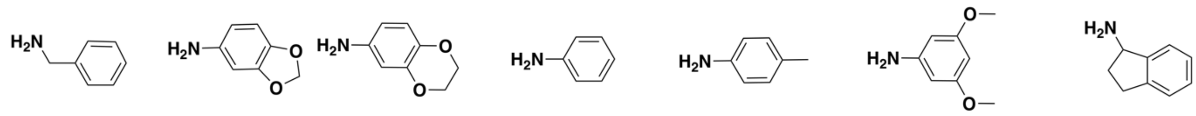

	J4	F5	F6	A1	A2	F4	N33
Expected mass (M - H+)	1069.5[a]	1115.5	1113.4	1055.4	1069.5	1115.5	1095.5
Experimental mass	1069.5	1115.5	1113.4	1055.4	1069.5	1115.5	1095.5
WT	0.000061	0.0039	0.0039	0.016	0.016	0.063	0.063
H481Y	>64	>64	64	>64	64	>64	>64
S486L	16	16	4	4	16	16	16

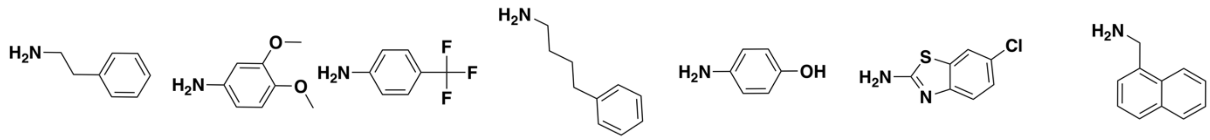

	C22	F3	N3	N8	A3	N5	C21
Expected mass (M - H+)	1083.5	1115.5	1123.4	1111.5	1071.4	1146.4	1119.5
Experimental mass	1083.5	1115.5	1123.4	1111.5	1071.4	1146.4	1119.5
WT	0.25	0.25	0.25	0.25	1	1	4
H481Y	>64	>64	>64	>64	>64	>64	>64
S486L	16	4	16	16	64	>64	>64

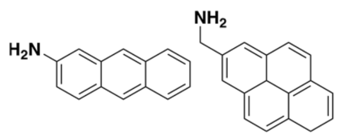

	N34	N35
Expected mass (M - H+)	1155.5	1195.5
Experimental mass	1159.5	1196.5
WT	4	4
H481Y	>64	>64
S486L	>64	>64

Round 2: J4 subscreen

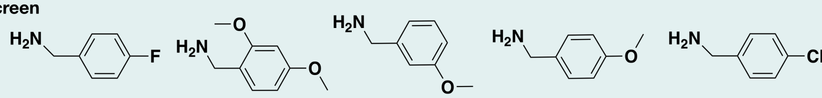

	N4	C13	F1	F2	N2
Expected mass (M - H+)	1087.4	1129.5	1099.5	1099.5	1103.4
Experimental mass	1087.4	1129.5	1099.5	1099.5	1103.4
WT	0.000061	0.0039	0.0039	0.0039	0.063
H481Y	>64	>64	>64	>64	>64
S486L	16	64	64	64	4

Figure S3. Complete collection of aromatic amines used in the synthesis of Kang amides. Aromatic amines were screened over two rounds of synthesis. The first round of synthesis broadly sampled this class of amines, while the second round utilized amines structurally related to J4, which yielded the most potent amide in the initial round of screening. The identity of each synthesized amide was verified by LC/MS. Expected and experimental masses are indicated. [a]The identity of J4, a lead compound for *in vivo* studies, was further verified by HRMS using a SCIEX X500B Q-TOF system: calcd *m/z* for $C_{57}H_{71}N_{2}O_{18}$ (M + H^{+}) 1071.4696, found *m/z* 1071.4654. MIC values (µg/mL) are shown for the amides generated from each amine against wild-type and rifampicin resistant (H481Y and S486L) *S. aureus* strains.

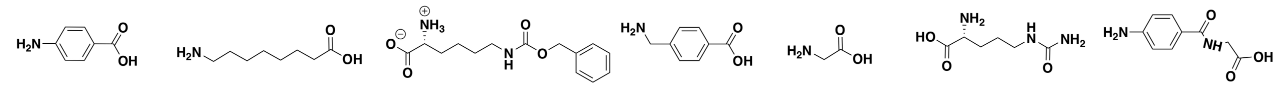

	N12	N17	N22	N13	N14	N18	N20
Expected mass (M - H⁺)	1099.4	1121.5	1242.5	1113.4	1037.4	1137.5	1156.5
Experimental mass	1099.4	1121.5	1242.5	1113.4	1037.4	1137.5	1156.5
WT	1	1	1	4	4	4	4
H481Y	>64	>64	>64	>64	>64	>64	>64
S486L	16	>64	>64	>64	>64	>64	>64

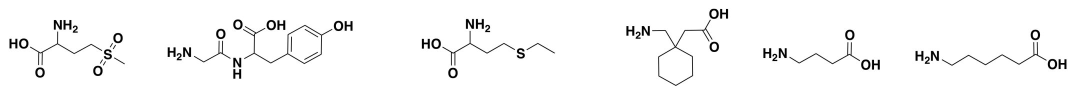

	N21	N23	N26	N27	N15	N16
Expected mass (M - H⁺)	1143.4	1200.5	1125.5	1133.5	1065.4	1093.5
Experimental mass	1143.4	1200.5	1125.5	1133.5	1065.4	1093.5
WT	4	4	4	4	16	16
H481Y	>64	>64	>64	>64	>64	>64
S486L	64	64	64	>64	>64	64

Figure S4. Complete collection of carboxylic acid amines used in the synthesis of Kang amides. The identity of each synthesized amide was verified by LC/MS. Expected and experimental masses are indicated. MIC values (μg/mL) are shown for the amides generated from each amine against wild-type and rifampicin resistant (H481Y and S486L) *S. aureus* strains.

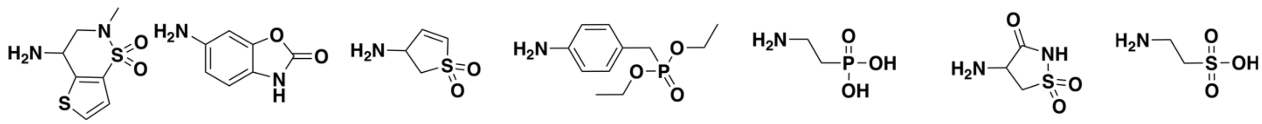

	P4	P5	P6	C16	P11	P3	P8
Expected mass (M - H+)	1180.4	1112.4	1095.4	1205.5	1087.4	1112.4	1087.4
Experimental mass	1180.4	1112.4	1095.4	1205.5	1087.4	1112.4	1078.4
WT	0.063	0.063	0.25	1	1	4	4
H481Y	>64	>64	>64	>64	>64	>64	>64
S486L	16	16	16	>64	4	64	64

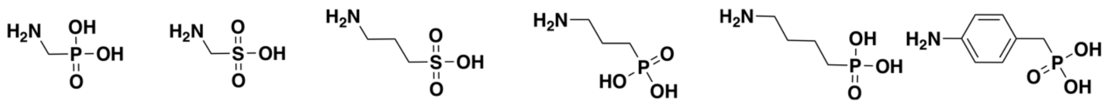

	P10	P7	P9	P12	P13	P14
Expected mass (M - H+)	1073.4	1073.4	1101.4	1101.4	1115.4	1149.4
Experimental mass	1073.4	1073.4	1101.4	1101.4	1115.4	1149.4
WT	4	16	16	16	16	16
H481Y	>64	>64	>64	>64	>64	>64
S486L	>64	>64	>64	>64	>64	>64

Figure S5. Complete collection of phosphate mimic amines used in the synthesis of Kang amides. The identity of each synthesized amide was verified by LC/MS. Expected and experimental masses are indicated. MIC values (μg/mL) are shown for the amides generated from each amine against wild-type and rifampicin resistant (H481Y and S486L) *S. aureus* strains.

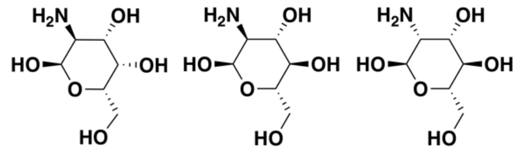

	C18	C19	S1
Expected mass (M - H⁺)	1141.5	1141.5	1141.5
Experimental mass	1141.5	1141.5	1141.5
WT	>64	>64	>64
H481Y	>64	>64	>64
S486L	>64	>64	>64

Figure S6. Complete collection of sugar amines used in the synthesis of Kang amides. The identity of each synthesized amide was verified by LC/MS. Expected and experimental masses are indicated. MIC values (μg/mL) are shown for the amides generated from each amine against wild-type and rifampicin resistant (H481Y and S486L) *S. aureus* strains*.*

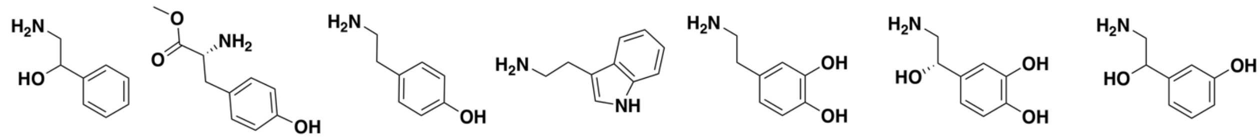

	C17	J3	A4	A5	A7	C14	C15
Expected mass (M - H+)	1099.5	1157.5	1099.5	1122.5	1115.5	1131.5	1115.5
Experimental mass	1099.5	1157.5	1099.5	1122.5	1115.5	1131.5	1115.5
WT	0.063	0.063	0.25	0.25	1	1	1
H481Y	>64	>64	>64	>64	>64	>64	>64
S486L	16	16	16	4	64	>64	64

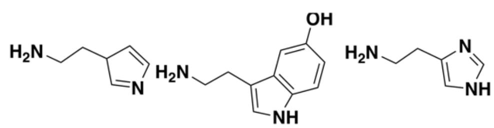

	P1	A6	P2
Expected mass (M - H+)	1072.5	1138.5	1073.5
Experimental mass	1072.5	1138.5	1073.5
WT	1	4	4
H481Y	>64	>64	>64
S486L	>64	64	>64

Figure S7. Complete collection of Phe/Trp/Tyr/His analogue amines used in the synthesis of Kang amides. The identity of each synthesized amide was verified by LC/MS. Expected and experimental masses are indicated. MIC values (µg/mL) are shown for the amides generated from each amine against wild-type and rifampicin resistant (H481Y and S486L) *S. aureus* strains.

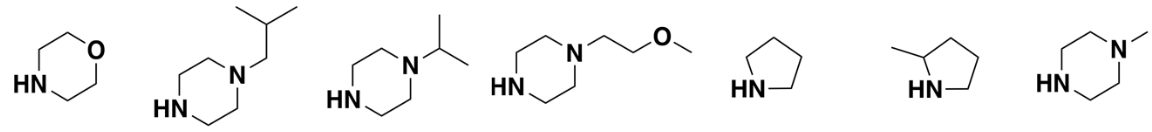

	C4z	KZ	Z6	Z8	N28z	N29z	Z5
Expected mass (M - H$^+$)	1170.5	1225.5[a]	1211.5	1227.5	1154.5	1168.5	1183.5
Experimental mass	1170.5	1225.5	1211.5	1227.5	1154.5	1168.5	1183.5
WT	0.0039	0.0039	0.0039	0.0039	0.016	0.016	0.016
H481Y	>64	16	16	>64	>64	64	>64
S486L	4	1	1	4	16	4	4

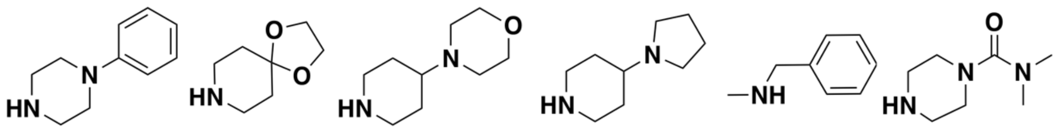

	Z7	Z10	Z11	N31z	Z4	Z9
Expected mass (M - H$^+$)	1245.5	1226.5	1255.6 (1096.5)[b]	1237.6	1204.5	1240.5
Experimental mass	1245.5	1226.5	1096.5	1237.6	1204.5	1240.5
WT	0.063	0.063	0.063	0.25	0.25	0.25
H481Y	>64	64	64	>64	>64	>64
S486L	16	4	16	16	16	16

Figure S8. Complete collection of amines used in the synthesis of C-3/C-4 Kang derivatives. The identity of each synthesized compound was verified by LC/MS. Expected and experimental masses are indicated. [a]The identity of KZ, a lead compound for *in vivo* studies, was further verified by HRMS using a SCIEX X500B Q-TOF system: calcd *m/z* for $C_{64}H_{83}N_4O_{20}$ (M + H$^+$) 1227.5595, found *m/z* 1227.5561. [b]LC/MS fragment of Z11 detected in positive ion mode (M + H$^+$). MIC values (µg/mL) are shown against wild-type and rifampicin resistant (H481Y and S486L) *S. aureus* strains.

Table S3. Comparison of bacterial burdens in mouse kidneys infected with *S. aureus* ATCC 12600 carrying an S486L RNAP mutation following treatment with KZ or Rif. Efficacy of compounds was evaluated in a neutropenic murine acute peritonitis/septicemia model. Infected mice received IP injections of drug (15 mg/mL) or vehicle (5% DMA plus 30% Captisol) at 2, 4 and 8 hours post infection. Bacterial burdens in kidneys were determined at 24 hrs post-infection. Limit of detection for burden quantification was calculated as 100 CFU/g of kidney. Log change in burden was calculated relative to the vehicle treated group.

Treatment	Mice	Average log CFU/g kidney	Average/Group	Log change in burden
Vehicle (5% DMA plus 30% Captisol)	1	4.9	5.7	0.0
	2	6.0		
	3*	5.8		
	4*	5.7		
	5	6.1		
	6*	5.6		
KZ (15 mg/kg)	1	3.8	3.8	-1.9
	2	3.6		
	3	4.0		
	4	3.7		
	5	3.9		
	6	4.1		
Rif (15 mg/kg)	1*	4.9	5.0	-0.7
	2*	4.9		
	3*	4.9		
	4*	5.0		
	5*	5.1		
	6	5.2		

*found dead at 24 hrs

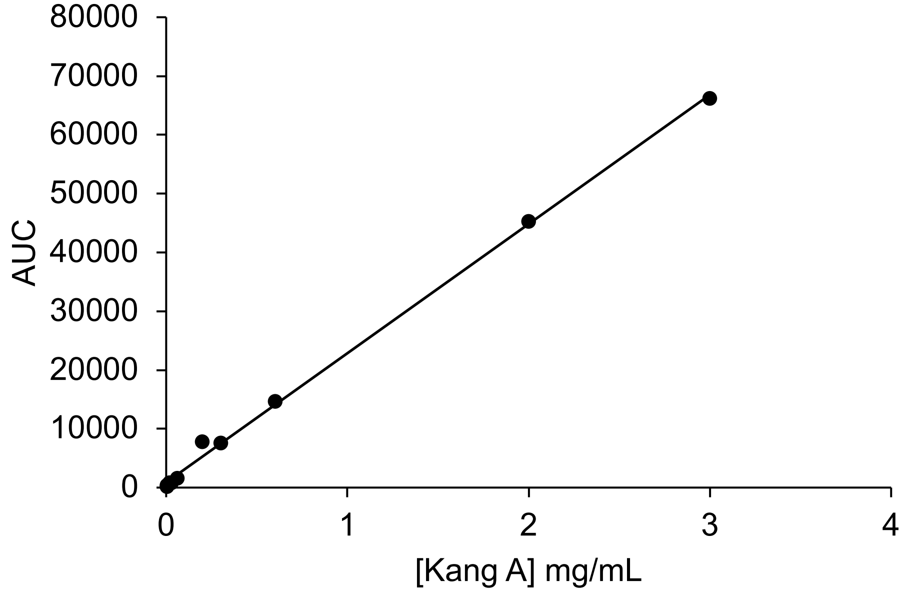

Figure S9. Calibration curve used to determine the concentration of Kang amides. Purified synthesized Kang amides were injected on a Waters Acquity H-Class UPLC and the UV absorbance of each compound was monitored at 395 nm. The area under the curve (AUC) for the UV peak corresponding to each compound was compared to the calibration curve shown above to determine the concentration (mg/mL) of each synthesized compound.

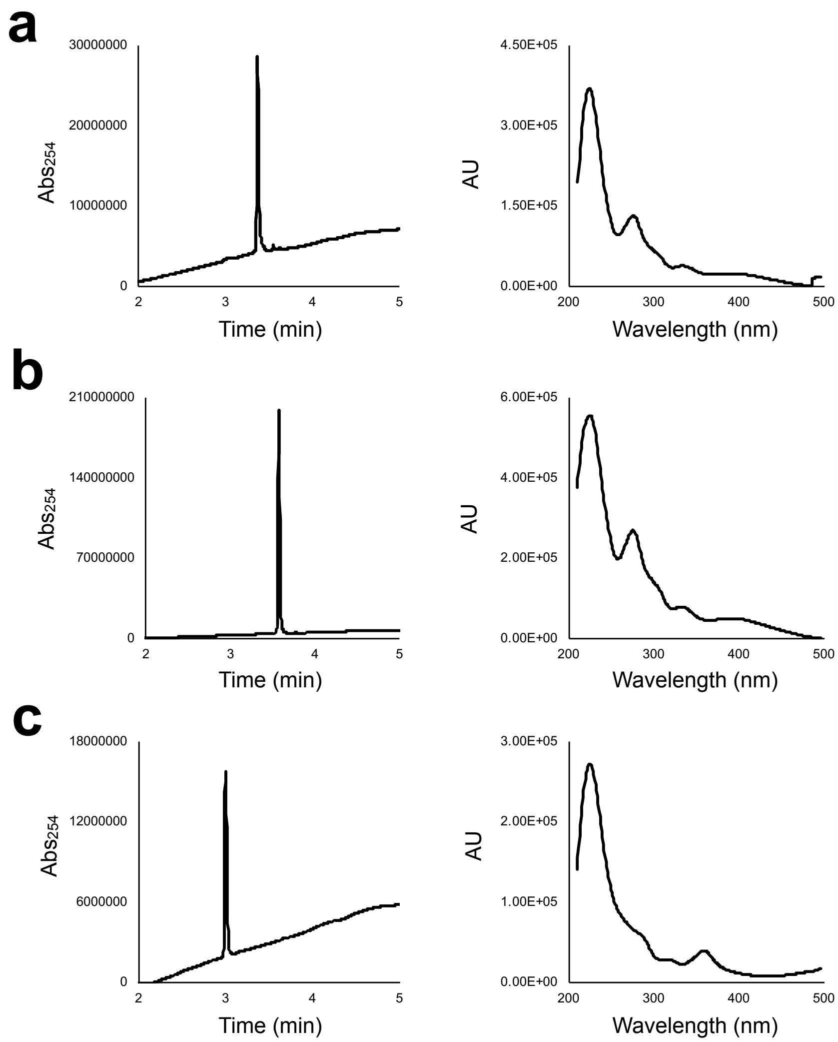

Figure S10. UPLC traces and UV spectra of purified a) Kang A, b) J4, and c) KZ. Compounds were analyzed using a Waters Acquity H-Class UPLC.

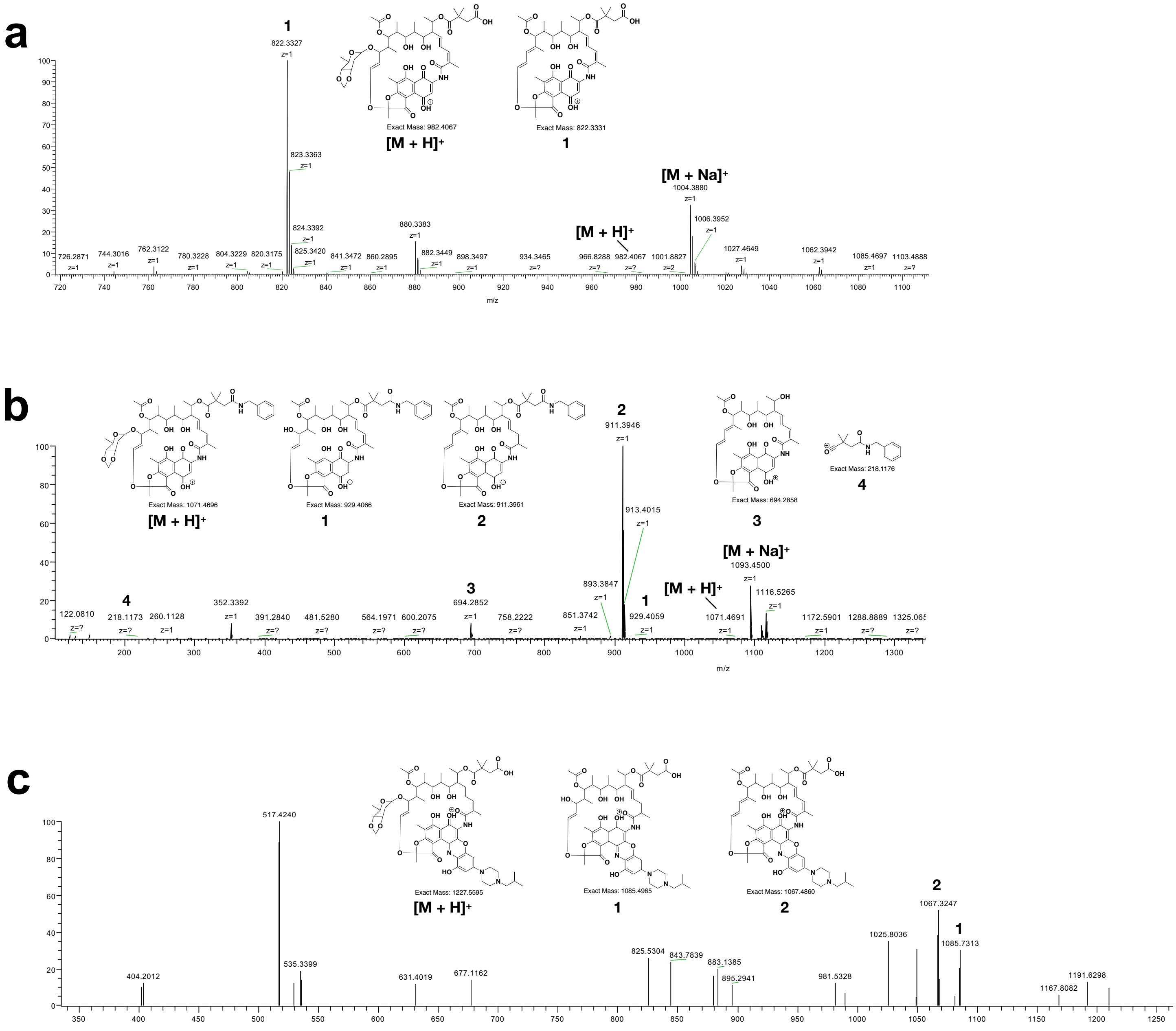

Figure S11. Mass fragmentation analysis of a) Kang A, b) J4, and c) KZ. Samples were analyzed by LC-MS/MS.

a

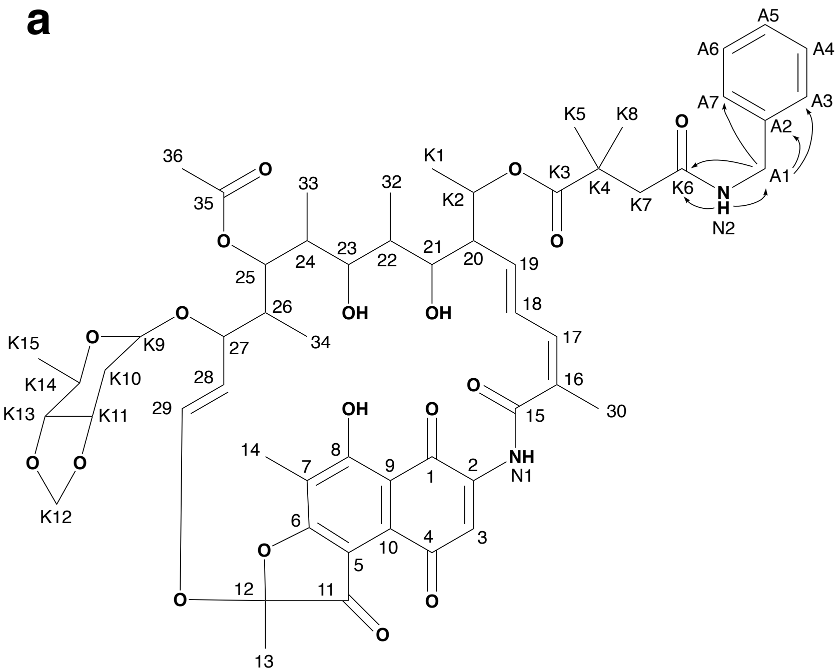

HRMS
Calculated *m/z* for $C_{57}H_{71}N_2O_{18}$ (M + H^+) 1071.4696
Found *m/z* 1071.4654

NMR correlations
⟶ **HMBC**

b

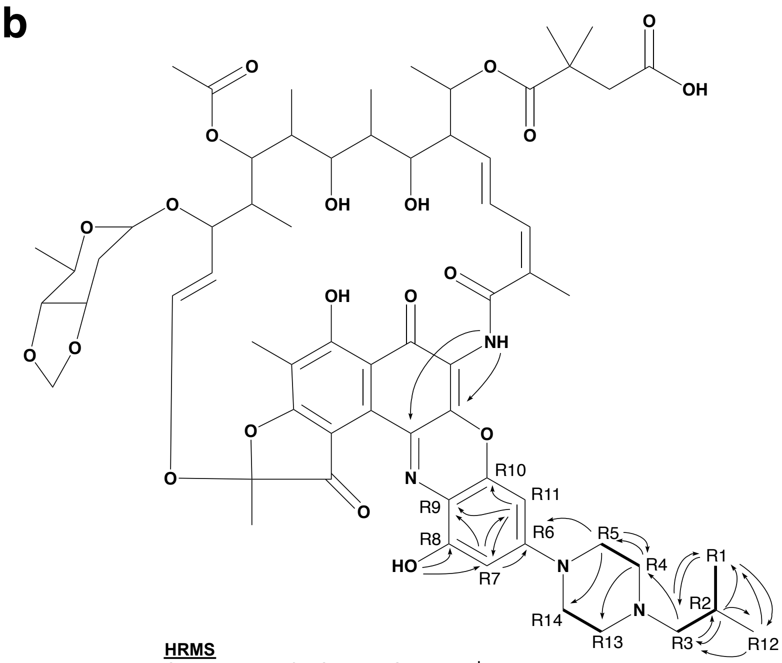

HRMS
Calculated *m/z* for $C_{64}H_{83}N_4O_{20}$ (M + H^+) 1227.5595
Found *m/z* 1227.5561

NMR correlations
⟶ **HMBC**
— **COSY**

Figure S12. HRMS and NMR data used to verify the structures of a) J4 and b) KZ.

Table S4. ^{1}H and ^{13}C chemical shifts of Kang A, J4, and KZ.[a]

	Kang A			J4[b]			KZ[b,c]		
Position	**Atom type**	**δ_C**	**δ_H (mult., *J* in Hz)**	**Atom type**	**δ_C**	**δ_H (mult., *J* in Hz)**	**Atom type**	**δ_C**	**δ_H (mult., *J* in Hz)**
1	C	185.8		C	184.9		C	181.9	
2	C	140.9		C	139.4		C	113.5	
3	CH	117.0	7.80 (s)	CH	117.5	7.72 (s)	C	128.9	
4	C	184.9		C	182.2		C	143.7	
5	C	111.7		C	111.1		C	104.8	
6	C	171.8		C	172.6		C	173.6	
7	C	116.9		C	115.8		C	107.9	
8	C	167.4		C	167.0		C	169.8[v]	
9	C	111.2		C	110.8		C	111.8	
10	C	132.0		C	130.8		C	130.7	
11	C	194.1		C	192.1		C	192.0	
12	C	109.9		C	108.0		C	106.1	
13	CH_3	23.7	1.67 (s)	CH_3	22.2	1.69 (s)	CH_3	22.2	1.69 (s)[m]
14	CH_3	7.8	2.34 (s)	CH_3	7.7	2.30 (s)[h]	CH_3	7.5	2.14 (s)[n]
15	C	171.6		C	170.9		C	171.0	
16	C	137.0		C	131.5		C	131.1	
17	CH	129.8	6.16 (d, 5.8)	CH	132.6	6.14 (d, 8.6)	CH	128.8	5.79 (m)[o]
18	CH	128.2	5.93 (dd, 15.9, 5.8)	CH	128.7	6.30 (dd, 15.9, 8.6)	CH	129.7	5.77 (m)[o]
19	CH	134.1	5.81 (dd, 15.9, 9.3)	CH	134.7	5.97 (dd, 15.9, 8.4)	CH	134.2	5.21 (t, 11.3)
20	CH	53.0	2.15 (m)[d]	CH	53.6	2.30 (m)[h]	CH	51.7	1.72 (m)[m]
21	CH	68.9	3.68 (m)[e]	CH	69.8	3.74 (d, 10.0)	CH	68.0	3.30 (m)
22	CH	33.8	1.84 (m)[f]	CH	33.2	1.78 (m)[i]	CH	31.5	1.62 (m)
23	CH	79.0	2.85 (dd, 10.0, 1.8)	CH	78.2	2.90 (10.1, 3.1)	CH	77.3	2.79 (t, 2.7)
24	CH	36.9	1.60 (m)	CH	37.4	1.47 (m)	CH	42.0	1.95 (m)[p]
25	CH	74.1	4.36 (dd, 9.5, 1.0)	CH	73.9	4.54 (d, 10.3)	CH	72.2	5.14 (br s)
26	CH	37.0	2.13 (m)[d]	CH	37.6	1.26 (m)[j]	CH	35.3	1.44 (m)
27	CH	81.5	3.85 (dd, 9.3, 2.7)	CH	78.8	3.82 (d, 5.9)	CH	78.2	3.54 (m)
28	CH	112.9	5.13 (dd, 12.8, 9.3)[g]	CH	115.9	5.06 (dd, 12.3, 6.5)	CH	111.4	4.91 (t, 10.3)
29	CH	146.4	6.37 (d, 12.8)	CH	144.4	6.27 (d, 12.3)	CH	142.5	5.85 (d, 11.8)
30	CH_3	21.1	2.06 (s)	CH_3	20.2	1.94 (s)	CH_3	20.8[w]	2.01 (s)
32	CH_3	12.9	0.94 (d, 7.0)	CH_3	12.5	0.98 (d, 7.0)	CH_3	11.1	0.83 (m)[q]
33	CH_3	9.4	0.69 (d, 6.7)	CH_3	9.5	0.60 (d, 6.7)	CH_3	11.9	0.83 (m)[q]
34	CH_3	13.4	0.38 (d, 7.2)	CH_3	11.2	0.18 (d, 7.1)	CH_3	12.4	0.56 (d, 5.1)
35	C	174.1		C	173.6		C	169.8[v]	
36	CH_3	21.8	2.02 (s)	CH_3	21.3	2.04 (s)	CH_3	20.9	1.94 (s)[p]
K1	CH_3	19.8	1.07 (d, 6.3)	CH_3	18.7	1.10 (d, 6.3)	CH_3	18.4	0.90 (m)[r]
K2	CH	68.0	5.06 (dd,12.7, 6.3)	CH	69.0	4.93 (dd, 12.2, 6.3)	CH	68.7	4.72 (m)
K3	C	176.4		C	176.6		C	175.1	
K4	C	40.8		C	43.5		C	40.0[z]	
K5	CH_3	26.2	1.17 (s)	CH_3	27.0	1.23 (s)[j]	CH_3	25.3	1.05 (s)
K6	C	172.3		C	170.5		C	172.0	
K7	CH_2	43.5	2.66 (d, 16.9)	CH_2	45.5	2.62 (d, 15.3)	CH_2	43.4	2.36 (d, 16.2)
			2.53 (d, 16.9)			2.45 (d, 15.3)			2.31 (d, 16.2)
K8	CH_3	24.9	1.23 (s)	CH_3	25.1	1.36 (s)	CH_3	24.3	1.07 (s)
K9	CH	97.2	4.65 (dd, 9.0, 1.1)	CH	98.0	4.50 (m)[k]	CH	96.7	4.47 (d, 3.5)
K10	CH_2	33.5	2.23 (ddd, 15.5, 2.9, 1.1)	CH_2	32.8	2.11 (dt, 14.6, 3.0)	CH_2	32.4	1.97 (m)
			1.83 (m)[f]			1.80 (m)[i]			1.80 (m)[s]
K11	CH	74.9	4.10 (m)	CH	74.0	4.01 (m)	CH	73.7	4.40 (m)
K12	CH_2	95.4	5.13 (s)[g]	CH_2	95.0	5.09 (s)	CH_2	94.6	5.04 (m)
			4.87 (s)			4.82 (s)			4.75 (m)
K13	CH	75.9	3.64 (m)[e]	CH	75.7	3.55 (dd, 9.0, 5.3)	CH	74.8	3.59 (dd, 8.8, 3.5)
K14	CH	70.5	3.36 (m)	CH	70.2	3.31 (m)	CH	69.3	3.23 (m)
K15	CH_3	18.8	1.27 (d, 6.2)	CH_3	18.7	1.24 (d, 6.2)[j]	CH_3	18.3	1.13 (d, 6.0)
N1	NH		8.34 (s)	NH		8.34 (s)	NH		9.30 (s)
N2				NH		6.60 (t, 5.1)			
OH-8	OH		12.60 (s)						
OH-R8							OH		9.86 (s)
J4-A1				CH_2	43.5	4.46 (m)[k]			
						4.26 (dd, 14.6, 5.1)			
J4-A2				C	138.7				
J4-A3				CH	128.0	7.23 (m)[l,x]			
J4-A4				CH	128.7	7.30 (m)[l,x]			
J4-A5				CH	127.4	7.27 (m)[l,x]			
J4-A6				CH	128.7	7.30 (m)[l,x]			
J4-A7				CH	128.0	7.23 (m)[l,x]			
KZ-R1							CH_3	20.8[w]	0.90 (m)[r]
KZ-R2							CH	24.8	1.83 (m)[s]
KZ-R3							CH_2	65.8	2.12 (m)[n]
									2.12 (m)[n]
KZ-R4							CH_2	52.8	2.48 (m)[t,y]
									2.48 (m)[t,y]
KZ-R5							CH_2	46.9	3.65 (br s)[u]
									3.65 (br s)[u]
KZ-R6							C	156.4	
KZ-R7							CH	94.0	6.51 (s)
KZ-R8							C	156.4	
KZ-R9							C	117.9	
KZ-R10							C	145.5	
KZ-R11							CH	91.3	6.77 (s)
KZ-R12							CH_3	20.8[v]	0.84 (m)[q]
KZ-R13							CH_2	52.8	2.48 (m)[t,y]
									2.48 (m)[t,y]
KZ-R14							CH_2	46.9	3.65 (br s)[u]
									3.65 (br s)[u]

[a] ^{1}H and ^{13}C NMR data were obtained at 600 and 150 MHz, respectively, at 25 °C on a Bruker Avance NMR with a TCI triple resonance cryoprobe. Solvents used were: CD_2Cl_2 (Kang A), $CDCl_3$ (J4), and DMSO-d_6 (KZ).

[b] Numbering of J4 and KZ carbon atoms is shown in Figure S12. Numbering of KZ carbon atoms has been modified from the numbering system for rifalazil presented in: Mae *et al*., Isolation and identification of major metabolites of rifalazil in mouse and human, *Xenobiotica*, 1999, 29, 1073-1087.

[c] KZ exhibited broad ^{1}H peaks in a number of common NMR solvents, possibly due to a conformational exchange process as previously reported for other benzoxazinorifamycins (Gill *et al*., Structure-based design of novel benzoxazinorifamycins with potent binding affinity to wild-type and rifampin-resistant mutant *Mycobacterium tuberculosis* RNA polymerases, *J Med Chem*, 2012, 55, 3814-3826). Low temperature experiments were attempted in an effort to improve the spectra, but were unsuccessful. The dataset presented here was collected at 25 °C in DMSO-d_6, which yielded the sharpest peaks of the conditions tested. While the presence of the KZ synthetic modification is apparent in the signals for KZ carbons R1 to R14 and their associated protons, the broadness of the proton peaks resulted in some ambiguity in multiplicity analysis and in peak assignments at other parts of the molecule.

[d-u] overlapping ^{1}H signals.

[v,w] overlapping ^{13}C signals.

[x,y] ^{1}H signal overlapped with solvent peak.

[z] ^{13}C signal overlapped with solvent peak.

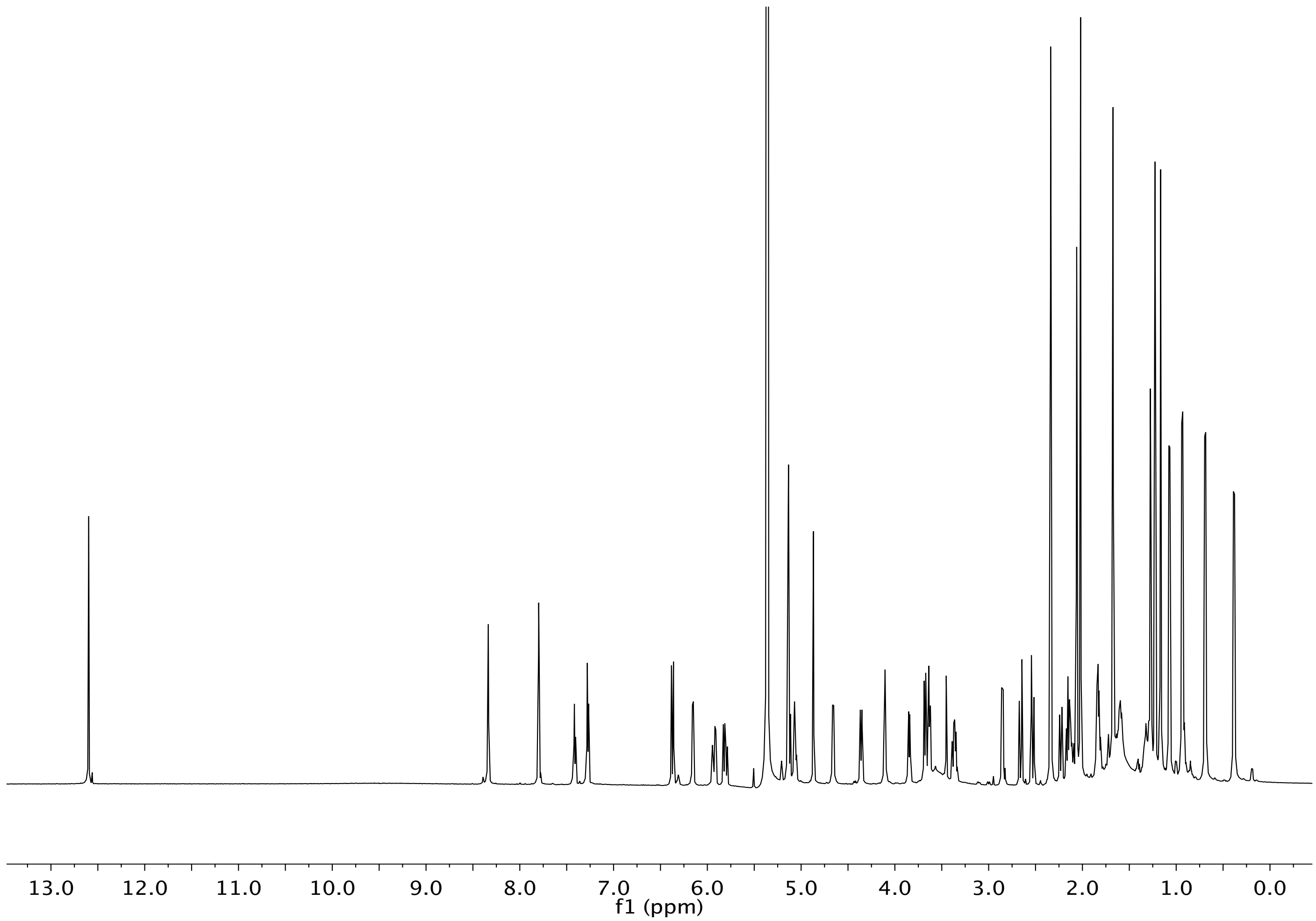

Figure S13. ^{1}H NMR spectrum of Kang A in CD_2Cl_2.

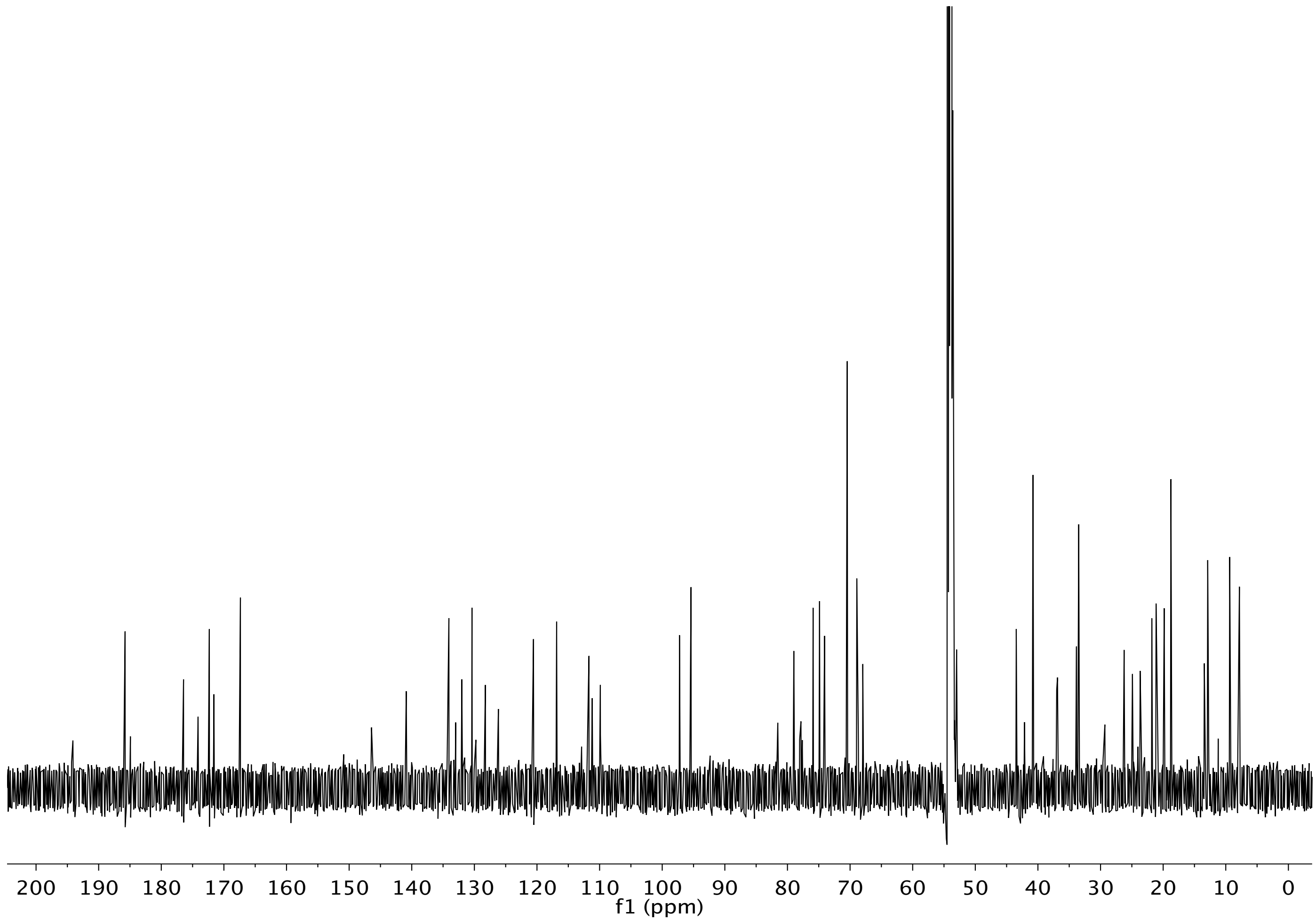

Figure S14. ^{13}C NMR spectrum of Kang A in CD_2Cl_2.

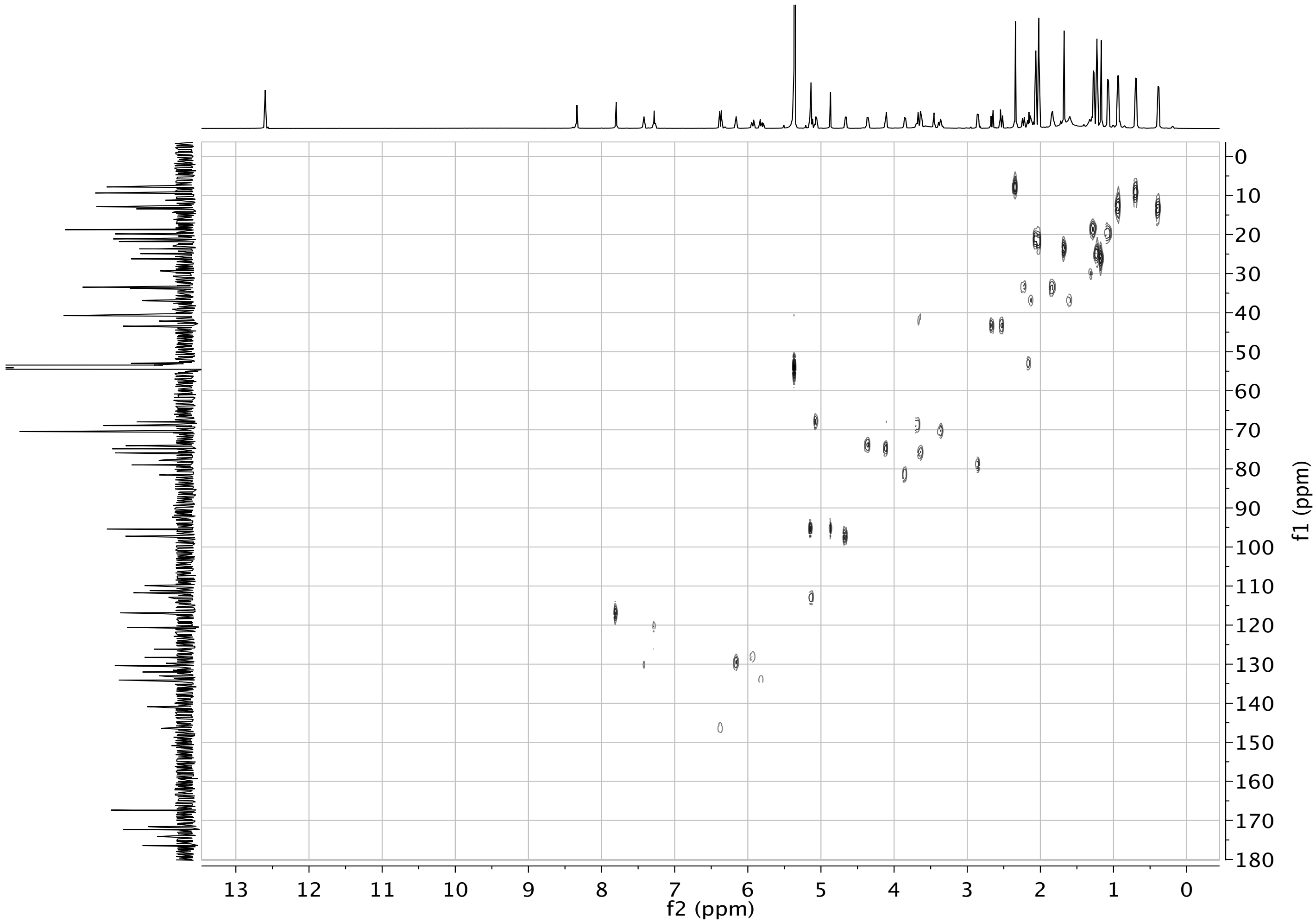

Figure S15. HMQC spectrum of Kang A in CD_2Cl_2.

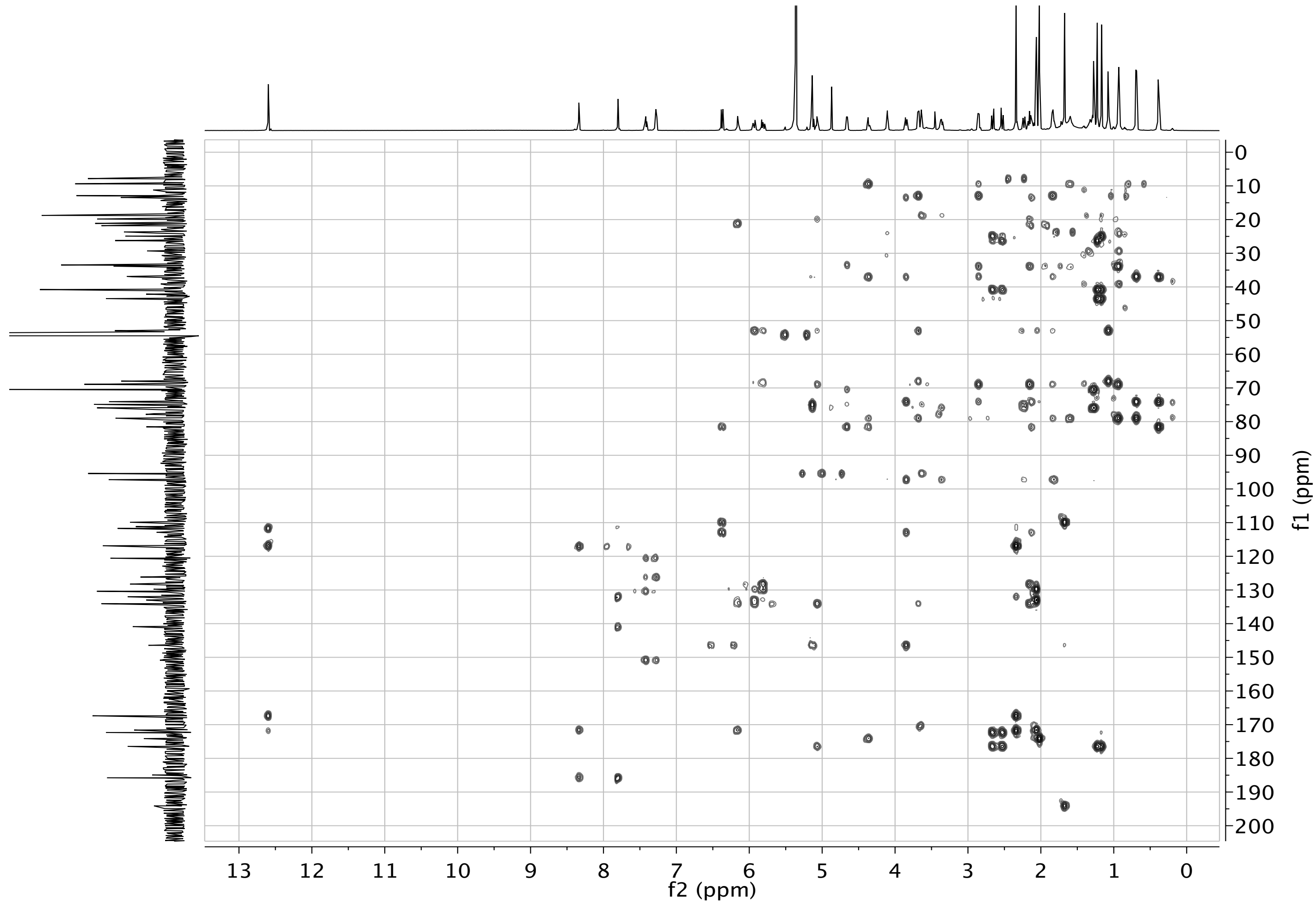

Figure S16. HMBC spectrum of Kang A in CD_2Cl_2.

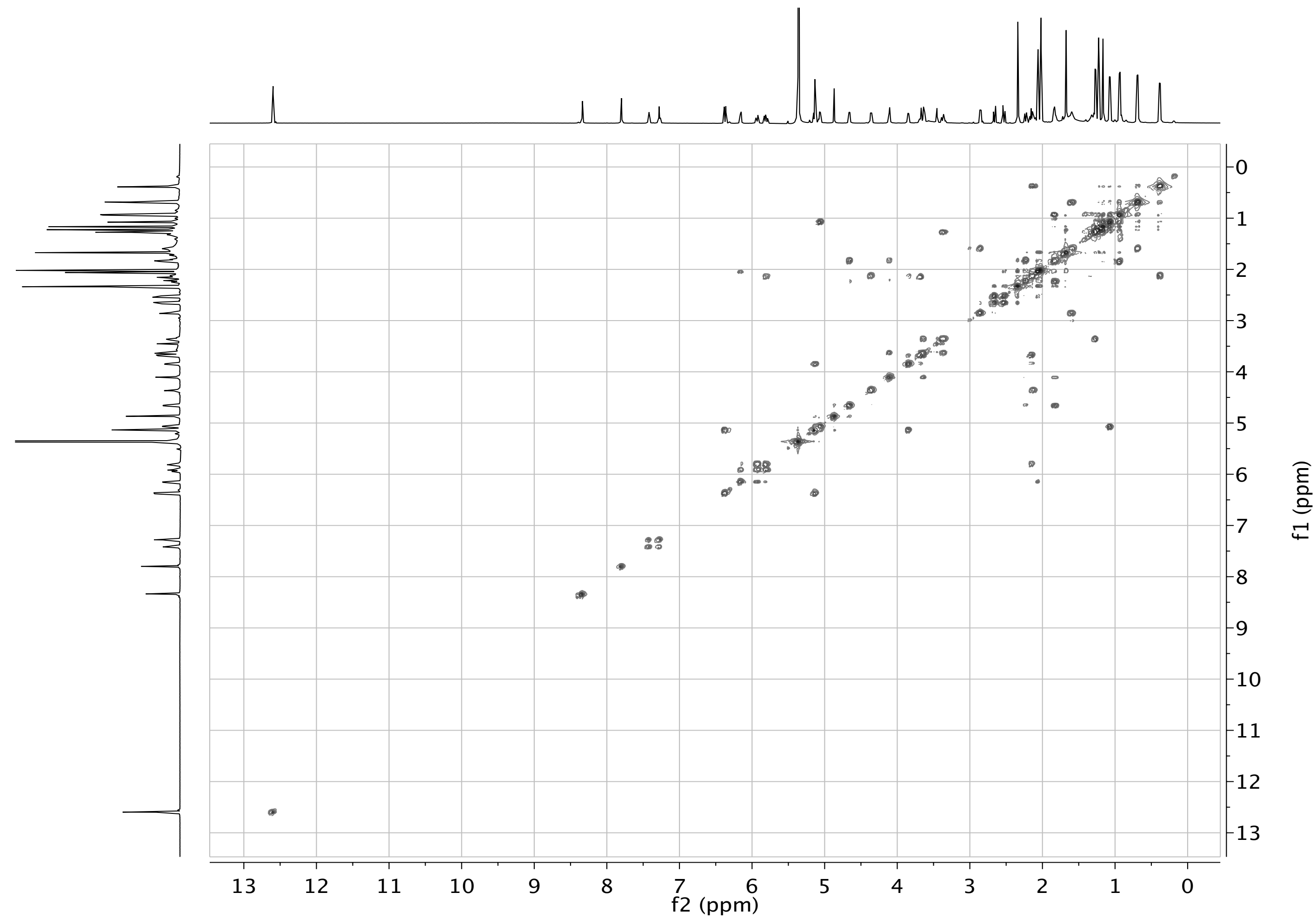

Figure S17. COSY spectrum of Kang A in CD_2Cl_2.

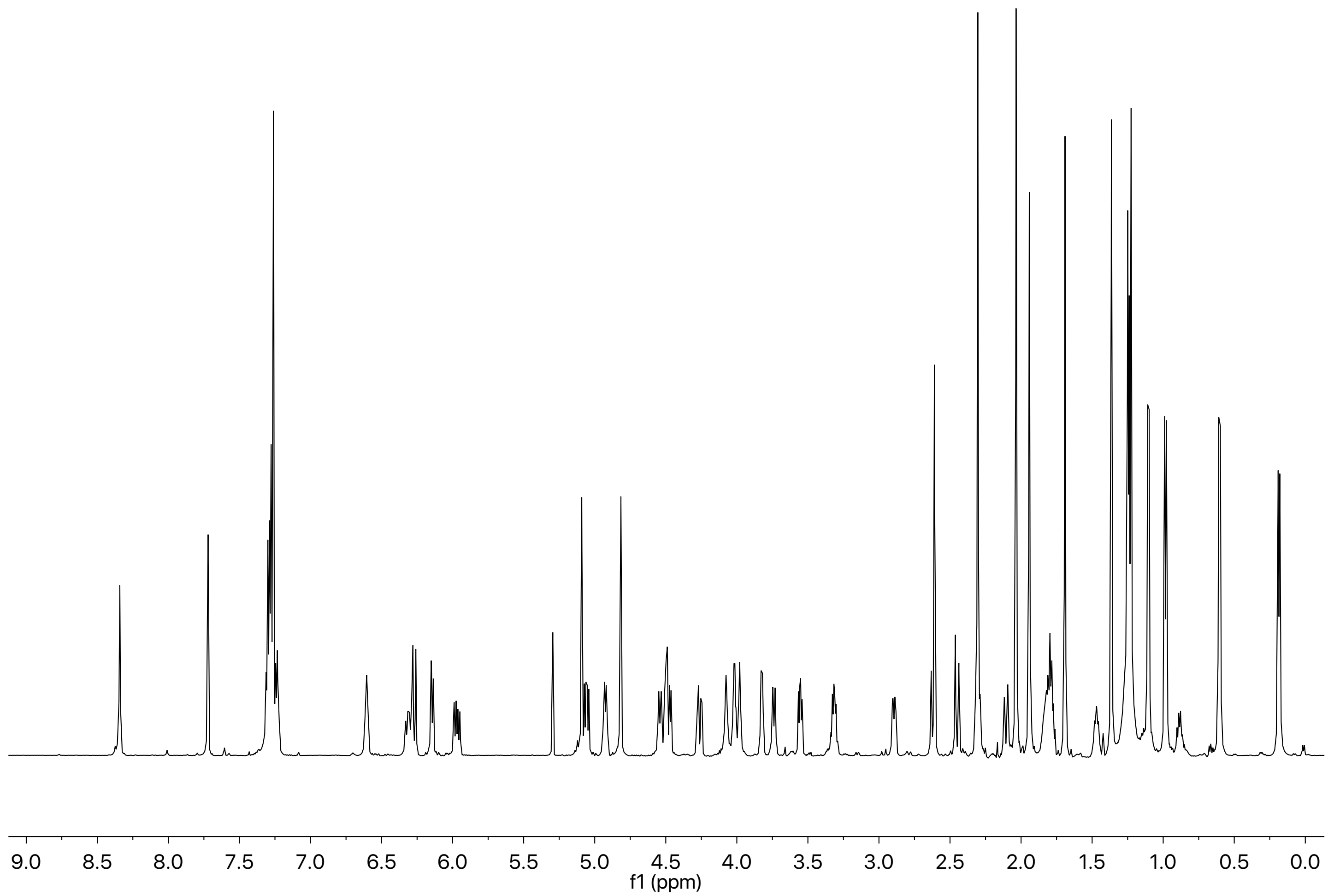

Figure S18. ^{1}H NMR spectrum of J4 in $CDCl_3$.

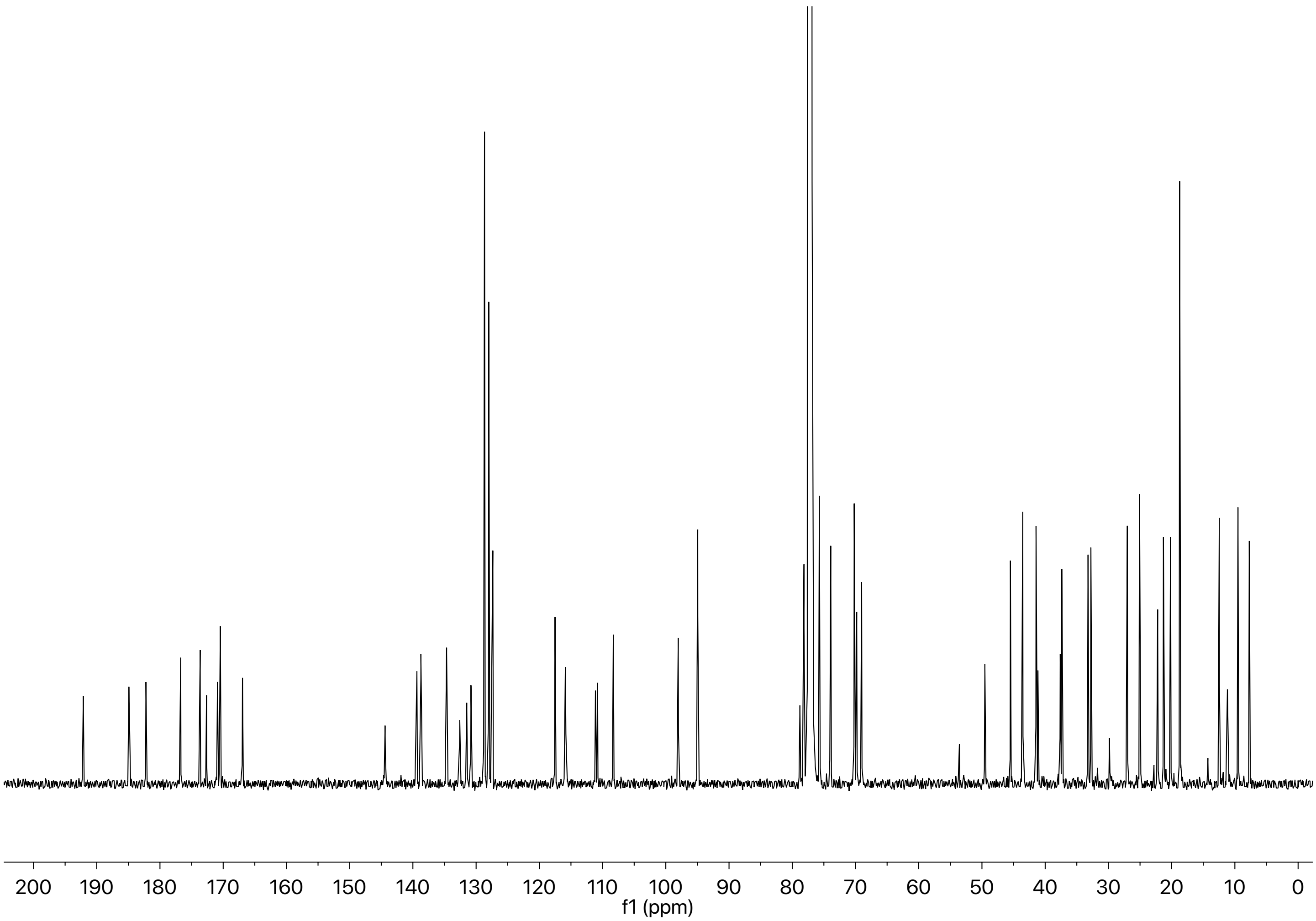

Figure S19. ^{13}C NMR spectrum of J4 in $CDCl_3$.

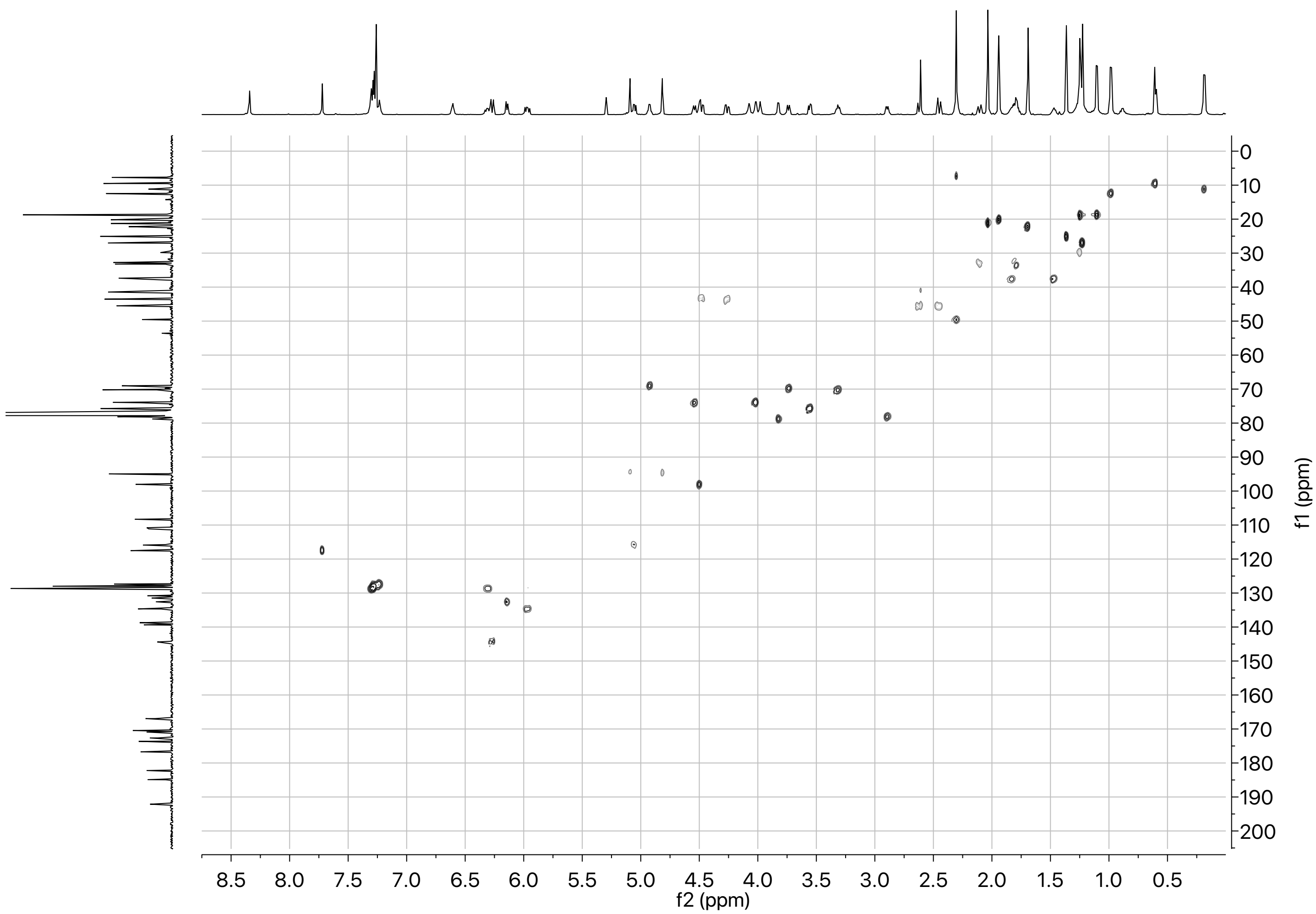

Figure S20. HSQC NMR spectrum of J4 in $CDCl_3$.

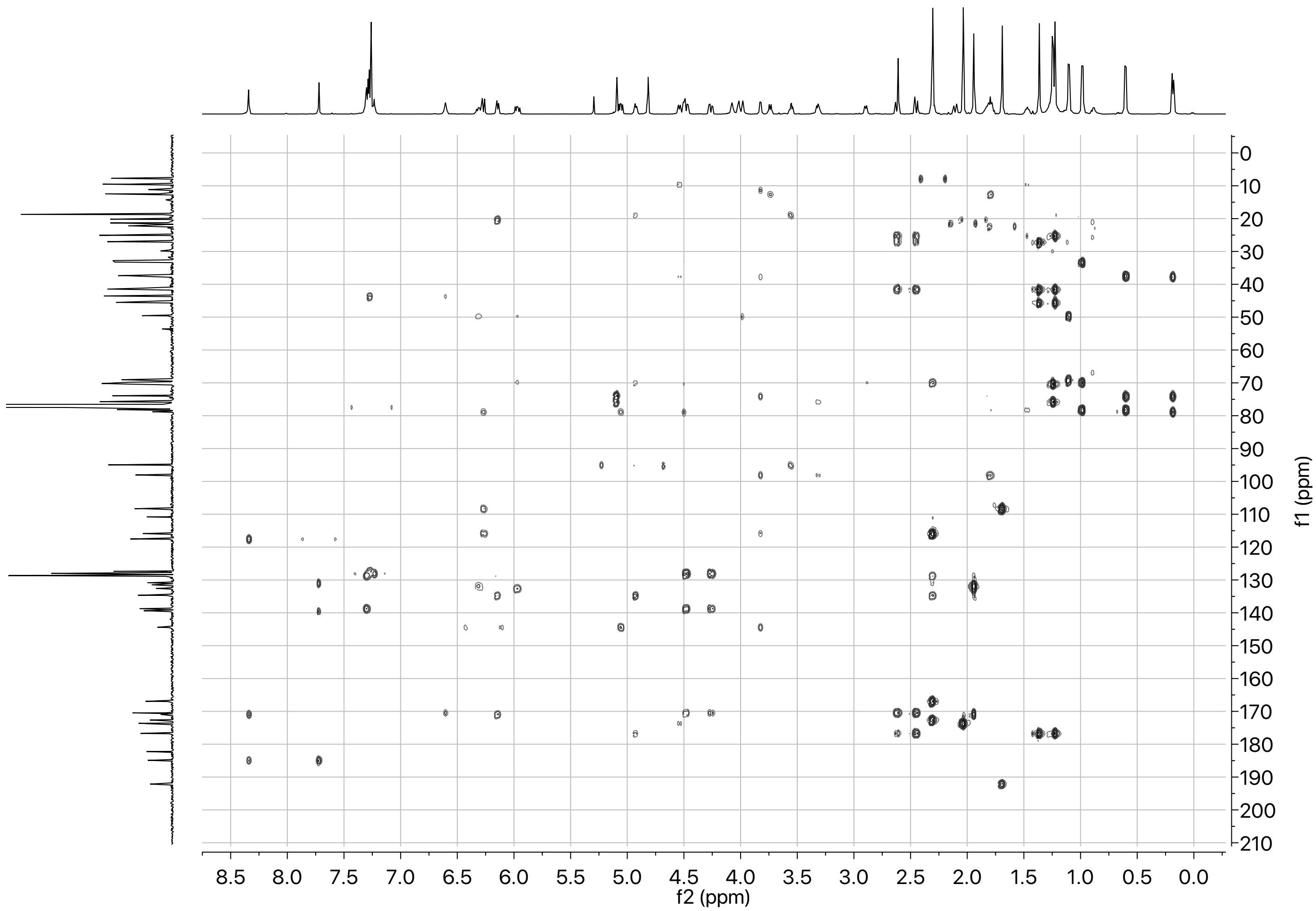

Figure S21. HMBC NMR spectrum of J4 in $CDCl_3$.

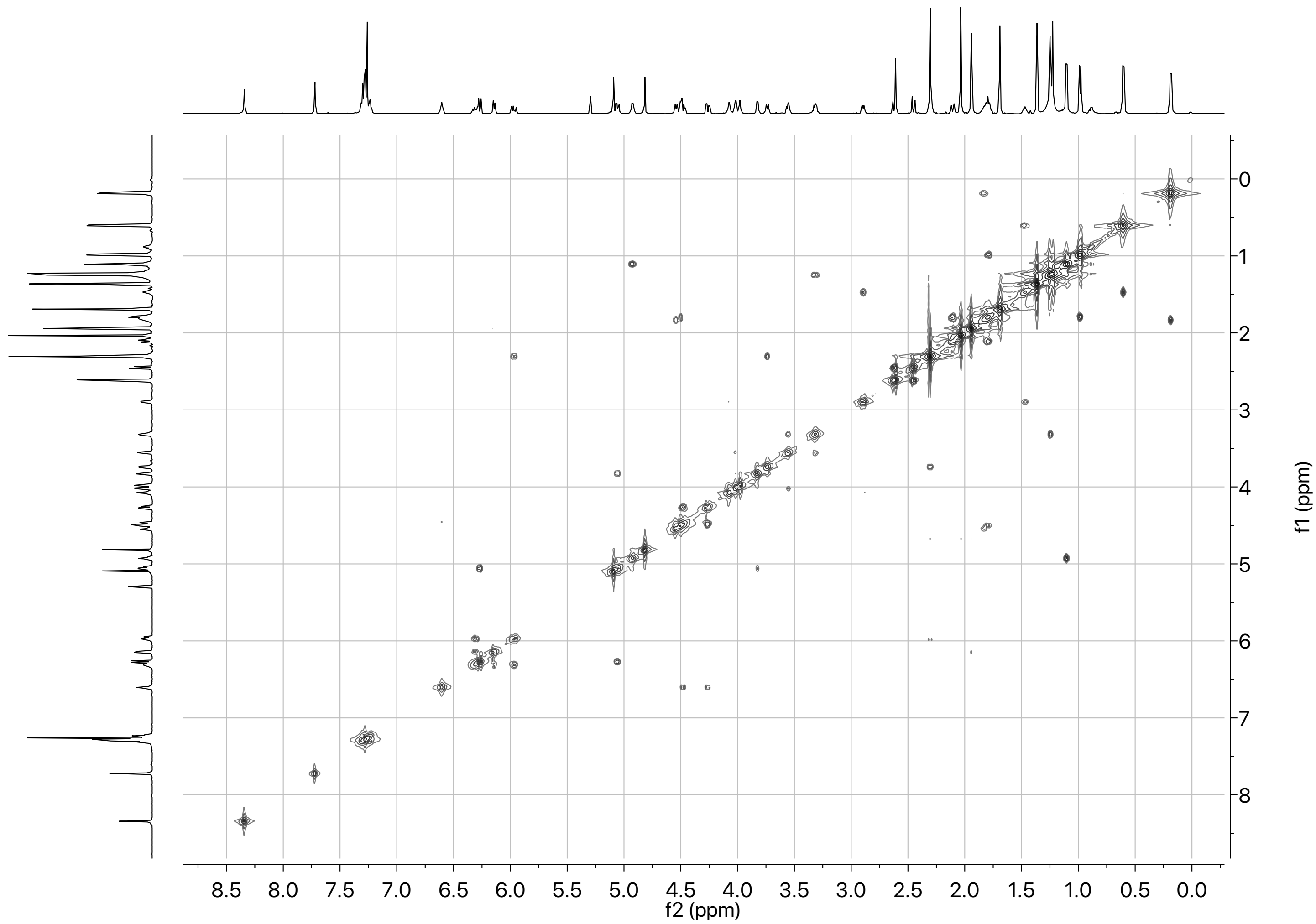

Figure S22. COSY NMR spectrum of J4 in $CDCl_3$.

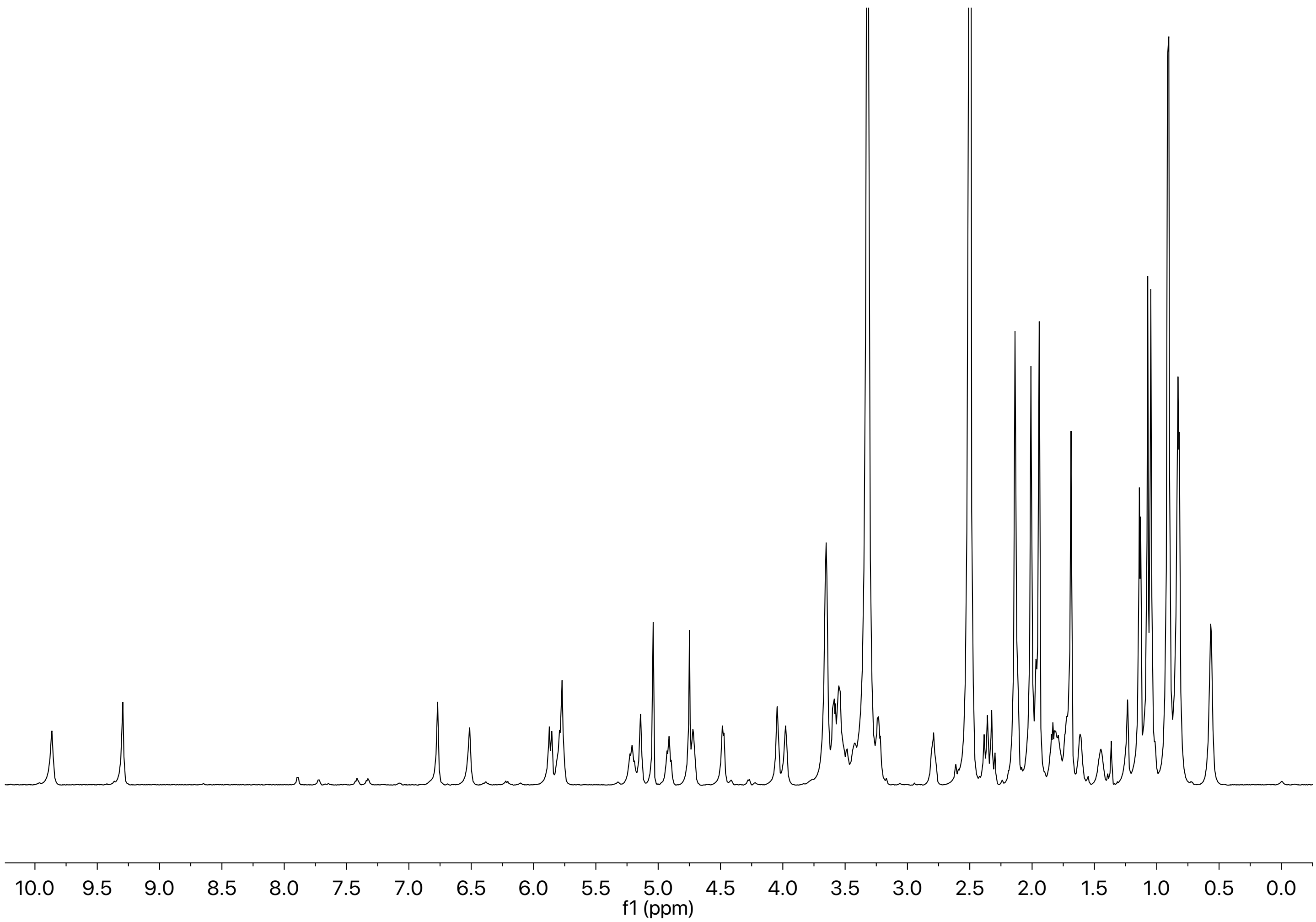

Figure S23. ^{1}H NMR spectrum of KZ in DMSO-d_6.

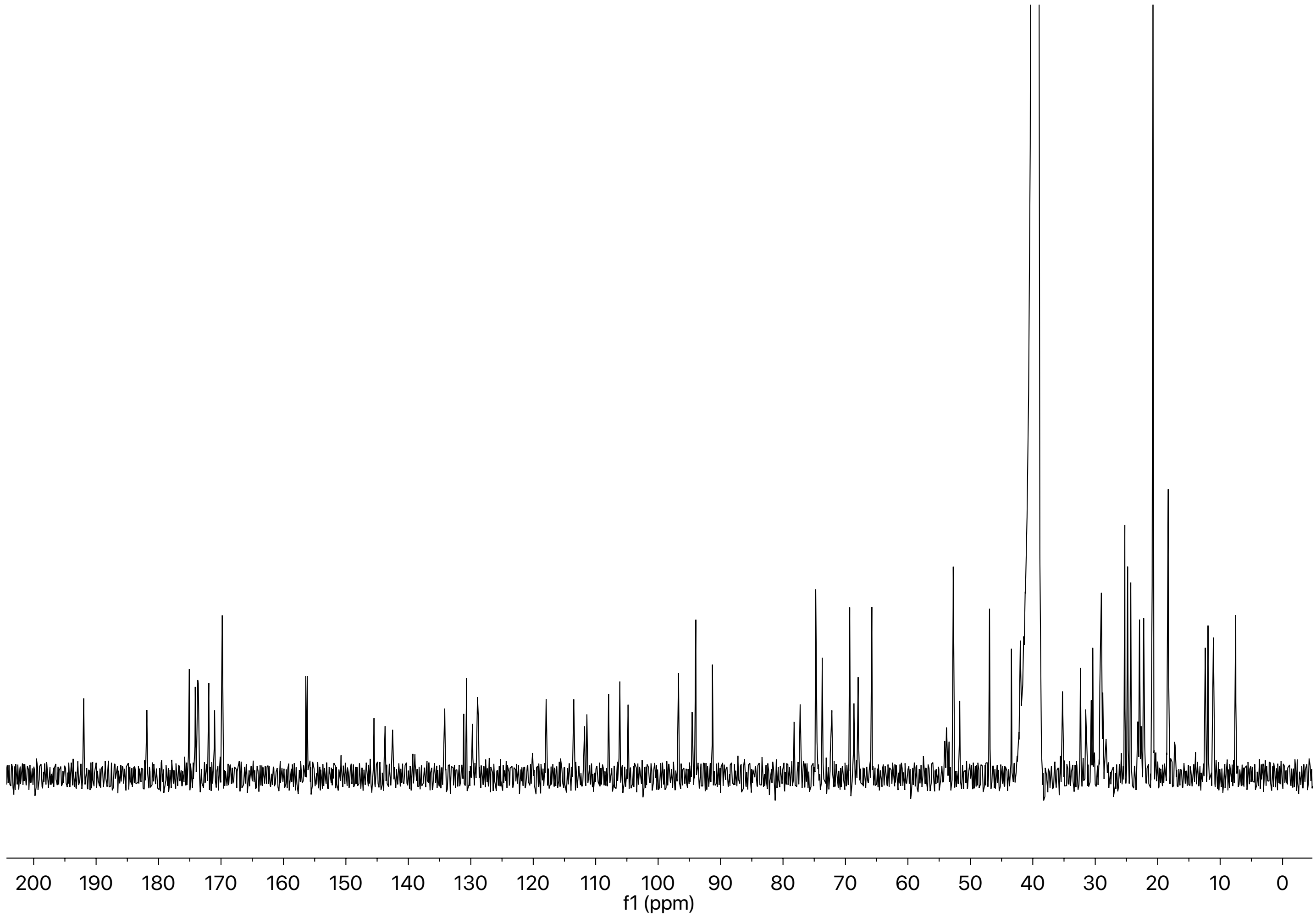

Figure S24. ^{13}C NMR spectrum of KZ in DMSO-d_6.

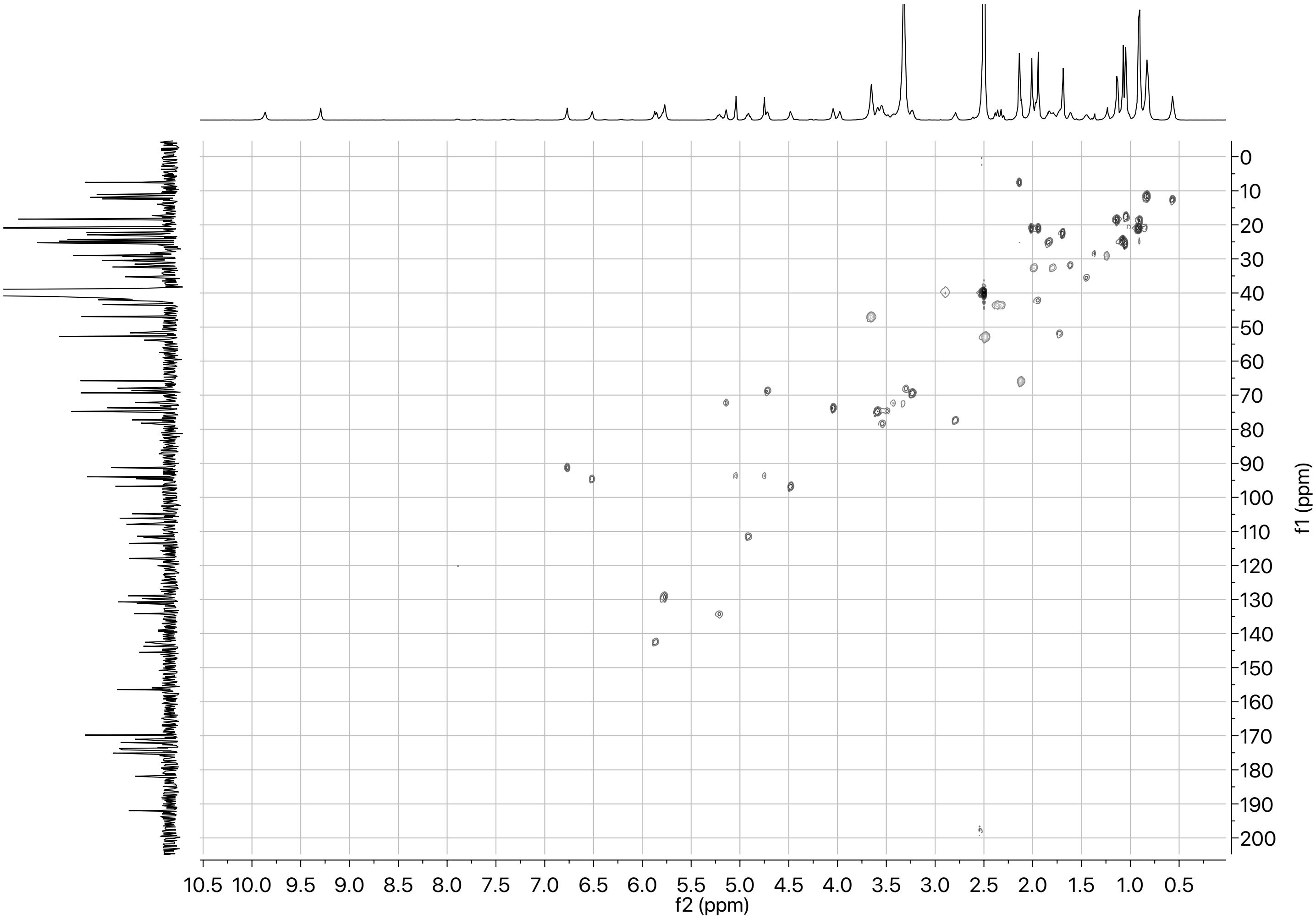

Figure S25. HSQC NMR spectrum of KZ in DMSO-d_6.

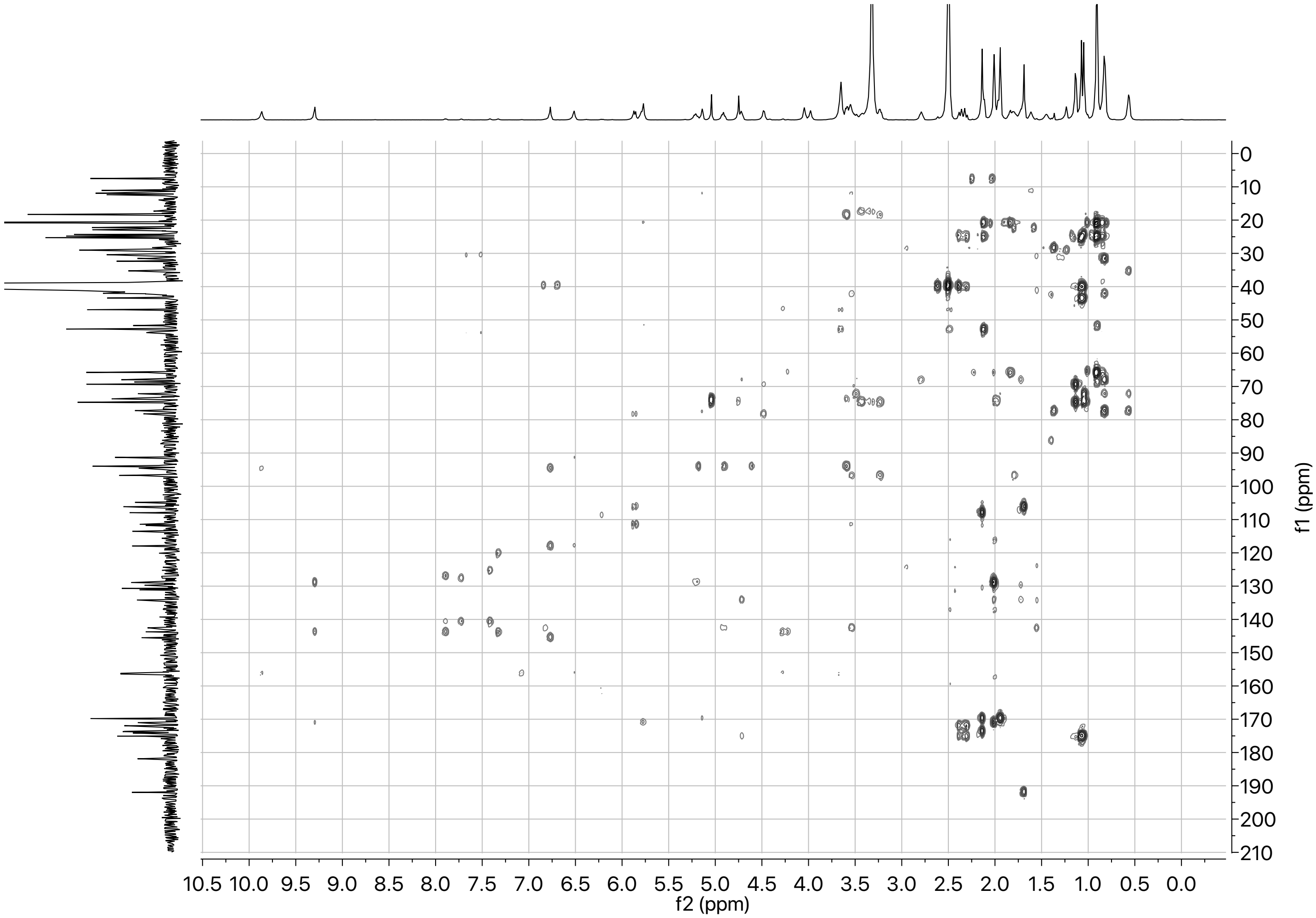

Figure S26. HMBC NMR spectrum of KZ in DMSO-d_6.

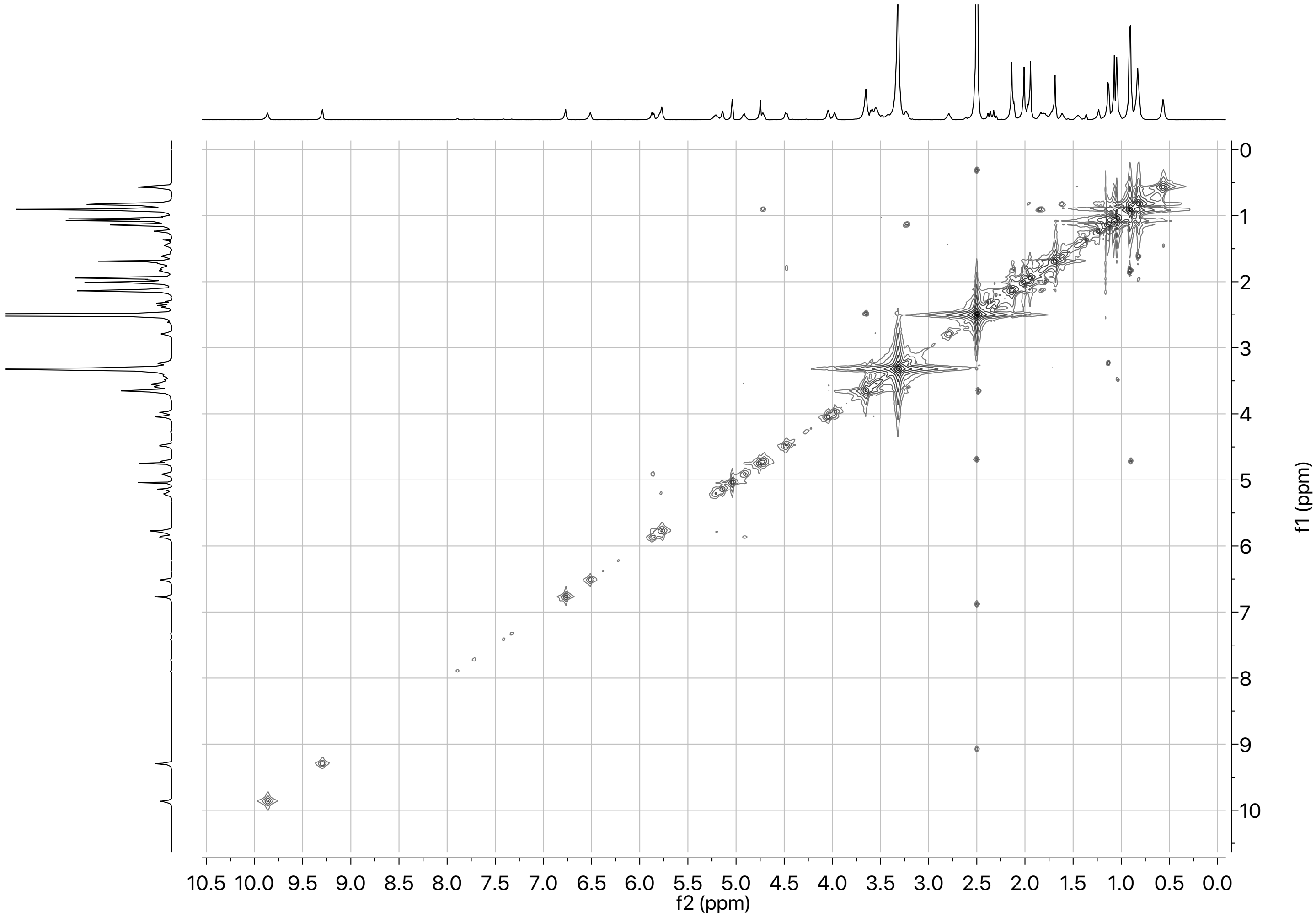

Figure S27. COSY NMR spectrum of KZ in DMSO-d_6.